

INFRARED DETECTING BEHAVIOURS OF $\text{Cu}_2\text{NiSnS}_4$ PHOTODIODES

Mustafa İLHAN¹, Mümin Mehmet KOÇ^{2*}

¹ *Department of Physics, Faculty of Literature and Science, Fırat University, Elazığ, TURKEY*

² *School of Medical Service, Kırklareli University, Kırklareli, TURKEY*

Abstract

A photodetector in Al/p-Si/Cu₂NiSnS₄/Al form was fabricated with sol-gel method. The structural assessment of the photodetectors was investigated and Cu₂NiSnS₄ structures were formed in nanostructure in granular form. Current–time and current-voltage investigations illustrated that Cu₂NiSnS₄ photodiodes have infrared sensing properties. Photodetection properties such as linear dynamic rate, ideality factor, photosensitivity and photoresponse characteristics were assessed. Results also validate the infrared sensing properties of the diodes. The barrier height of the Cu₂NiSnS₄ diodes is calculated as 0.466 eV. Ideality factor of the diodes was found to be 5.16. Results indicate that our Cu₂NiSnS₄ photodetectors are suitable for infrared tracking device applications.

Keywords: Quaternary Functional Photodetectors; Infrared Detectors; Photodiodes; Photodetectors

Öz

Al/p-Si/Cu₂NiSnS₄/Al yapıdaki fotodedektörler sol-jel yöntemi kullanılarak üretilmiştir. Taramalı elektron mikroskobu (SEM) kullanılarak fotodedektörler yapısal olarak incelenmiştir. Mikroskopik incelemeler sonucunda Cu₂NiSnS₄ yapının nanoformda sentezlendiği ve nanoparçacıkların granüler yapıda bir arada bulunduğu gözlemlenmiştir. Akım – zaman ve akım - voltaj grafikleri Al/p-Si/Cu₂NiSnS₄/Al yapıda üretilmiş olan diyotlarımızın kızılötesini ışığı hissedebilme özellikleri gösterdiğini göstermiştir. Fotodedektör özelliklerini incelemede kullanılan lineer dinamik oran, idalite faktörü, fotohassasiyet, fototepki karakteristikleri gibi karactersistik özellikler çalışmamızda detaylıca incelenmiştir. İncelenen fotodiyot karakteristikleri de fotodiyotlarımızın kızılötesi dedektör özellikleri gösterdiğini doğrulamıştır. Al/p-Si/Cu₂NiSnS₄/Al yapıdaki diyotlarımıza ait bariyer yüksekliği 0.466 eV olarak hesaplanırken idealite faktörü ise 5.16 olarak bulunmuştur. Sonuçlar incelendiğinde Al/p-Si/Cu₂NiSnS₄/Al yapıda üretilmiş fotodiyotların infrared tarama cihazlarında kullanılmaya uygun olduğu anlaşılmaktadır.

Anahtar Kelimeler: Dört Bileşenli Fonksiyonel Fotodedektörler; Kızıl Ötesi Dedektörleri; Fotodiyotlar; Fotodedektörler

* Corresponding Author: muminmehmetkoc@klu.edu.tr

1. INTRODUCTION

Photodiodes constitute the essential parts of photodetector and photosensor applications. Photodetectors and photodiodes were used in different types of technological implications. Therefore, scientists from different areas like physics, engineering, chemistry, materials engineering and science investigate the structural, electrical and optoelectronic properties of the photodiodes. Different materials can be used in the fabrication of photodetectors and photodiodes. Organic based molecules were often considered as fabrication materials, since they are easy to synthesize and abundant in the nature [1]–[3]. However, organic material based devices have some drawbacks such as instability, fragility and short lifetime [4], [5]. Therefore, different alternatives were applied. For example, organic material based photodiodes were often produced in composite forms or doped with other materials such as nanoparticles [1], [6]. It was evidenced by different papers that such a solution enhance mechanic, electric and optoelectronic properties of the photodiodes [7]–[9]. On the other hand, metallic thin film based photodiodes were found to be more reliable. Since, they are not easily affected by external factors, they are more durable, and they have astonishing electrical and optoelectronic properties. Hence, electric, electronic and magnetic properties of the metallic based diodes subject to an active research in the literature [10]–[14]. In addition, producing thin films in composite form and doping metallic thin films with other molecules help researchers to adjust the electrical properties of the metallic photodetectors [11], [15]–[19]. Thin films have relatively low energy band gap and good photoresponsive properties [20], [21]. Quaternary functional photodetectors have a special role [15] among the metallic based photodetectors. Quaternary functional photodetectors have a thin film layer which consist of four different material [22]. Quaternary functional photodetectors in different forms were reported in the literature. $\text{Cu}_2\text{NiSnS}_4$, $\text{Cu}_2\text{CoSnS}_4$ and $\text{Cu}_2\text{ZnSnS}_4$ structures are popular structures reported in the literature. Electrical properties of such structures were detailly investigated [23]–[26]. It was evidenced that such structures have strong potential to be used as infrared detectors [27], [28]. Previously HgCdTe structures were considered as infrared detectors [29]. However, HgCdTe structures have lattice mismatch problem [30]. The problem strongly affects the device quality

mechanical properties of the infrared diodes. CdTe buffer layers were proposed to overcome such a drawback [30], [31]. However, CdTe buffer layers alter the electrical and optoelectronic properties of the HgCdTe structures. At this point, quaternary functional structures step forward. In this work, we produced Al/p-Si/Cu₂NiSnS₄/Al diodes to assess their infrared sensing properties. Sol-gel method was used in the production of Cu₂NiSnS₄ active layer which was found to be in nanostructure form. Such method was cheap, reliable, and facile. I-V and I-t properties were assessed under infrared illumination. Photocharacterization of the photodiodes were performed. Photoresponse, photosensitivity, ideality factor, barrier height characteristics were also assessed under infrared illumination. It was concluded that photodiodes were reflects infrared sensing properties.

2. MATERIALS AND METHOD

Sol-gel technique was used in the production of infrared active Cu₂NiSnS₄ nanoparticles which were used in the core of the device. Before the production of Cu₂NiSnS₄ thin films. Cleaning procedures were applied to the Si wafers [32]. P-type Si substrate was used as the main platform of the device. Firstly, p-type Si wafers were rinsed with pure water and sonication procedure was applied for 5 mins in acetone. Wafer was rinsed and sonicated in pure H₂O. Si substrates were etched in HF:H₂O (1:10 ml) for 30 sec [32]. After the etching, Si substrates were rinsed in sonic bath. Al contact was applied to the one side of p-type Si substrate. Al/p-Si structure is heated at 570 °C. After annealing procedure Al/p-Si structure was rinsed. 2 m mol CuCl₂, 1m mol SnCl₂, 5 m mol CH₄N₂S (Thiourea) and 1m mol NiCl₂ were poured to 80ml DMF (Dimethylformamide). Mixture stirred at 500 rpm. Mixture was then poured in hydrothermal nanoparticle synthesis device where it was kept there for 24 h at 250 °C. To take the sediment from the result product, mixture was centrifuged. Drained sediment was dried and obtained nanopowders were used in the coating process. Cu₂NiSnS₄ nanoparticles were dissolved in chlorobenzene. Chlorobenzene dissolved mixture was dropwise placed on Al contacted Si substrate. Spin coating process was performed. As a result, fabrication of Al/p-Si/Cu₂NiSnS₄ structure was completed. Al/p-Si/Cu₂NiSnS₄ structure was heat treated to dry the excessive liquids. Finally, Al coating was performed and where Al/p-Si/ Cu₂NiSnS₄/Al quaternary functional photodiode fabrication was completed. FYTRONIX

FY-INF1000 infrared characterization system was used in the device characterization. Karl Zeiss SEM was used in the microscopic investigations of the surface.

3. RESULT AND DISCUSSION

Figure 1 illustrates the SEM (Scanning Electron Microscopy) results of $\text{Cu}_2\text{NiSnS}_4$ quaternary functional photodiodes. Images obtained in 15 K (a) and 150 K (b) magnification; they were illustrated in Figure 1. Figure shows the nanostructures which form the active layer of Al/p-Si/ $\text{Cu}_2\text{NiSnS}_4$ /Al quaternary functional photodiodes. It was seen that active layer consists of $\text{Cu}_2\text{NiSnS}_4$ nanostructures which was in granulated shape where nanoparticles agglomerate and forms big lumps. Size of $\text{Cu}_2\text{NiSnS}_4$ nanoparticles were found to be between 200 nm – 500 nm. It was also understood that nanoparticles have narrow size distribution.

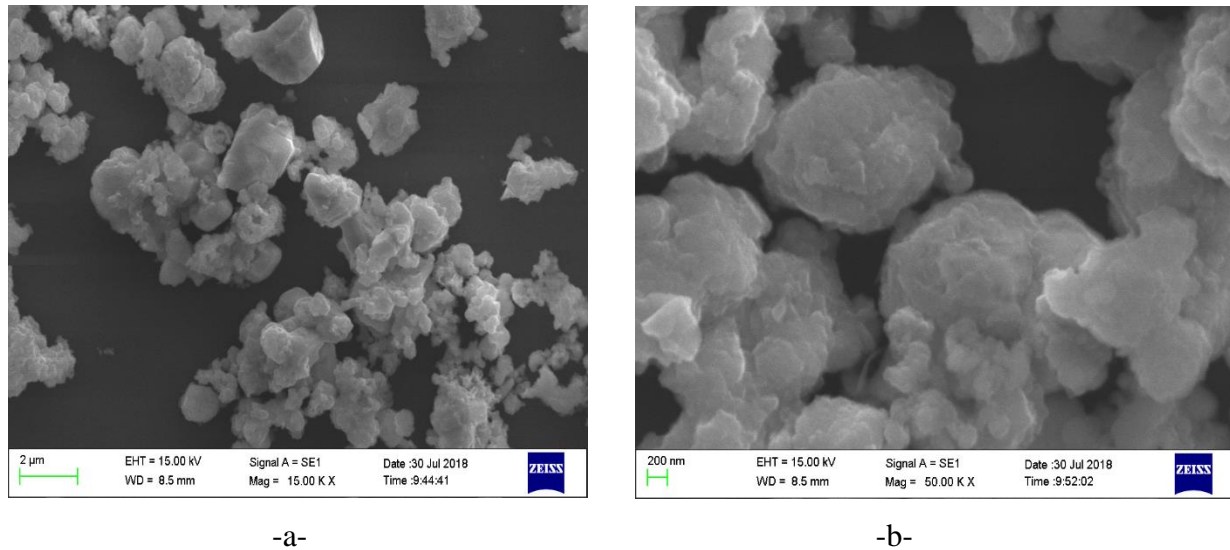


Figure 1: SEM images of $\text{Cu}_2\text{NiSnS}_4$ obtained under 15K (a) and 50K (b) magnification.

To evaluate the electronic characteristics of $\text{Cu}_2\text{NiSnS}_4$ quaternary functional photodetectors, current-time (I – t) and current-voltage (I – V) behaviors were investigated. Various illumination intensities were used in the assessment of current-voltage characteristics. I-V behaviors of the $\text{Cu}_2\text{NiSnS}_4$ quaternary functional photodetectors were assessed between +3 V and -3 V. Only infrared illumination was used in the assessment. Current-voltage behaviors were given in Figure 2. Figure illustrates that Al/p-Si/ $\text{Cu}_2\text{NiSnS}_4$ /Al quaternary functional photodiodes respond to

infrared light. Noticeable difference between dark measurement and measurements obtained under infrared illumination was seen. It was noticed that enhanced infrared illumination enhances the measured current in the backward bias region. Slight barrier voltage difference between dark measurement and infrared illumination measurement can be identified in the figure. Enhanced barrier voltage difference was seen for enhanced infrared illumination intensities.

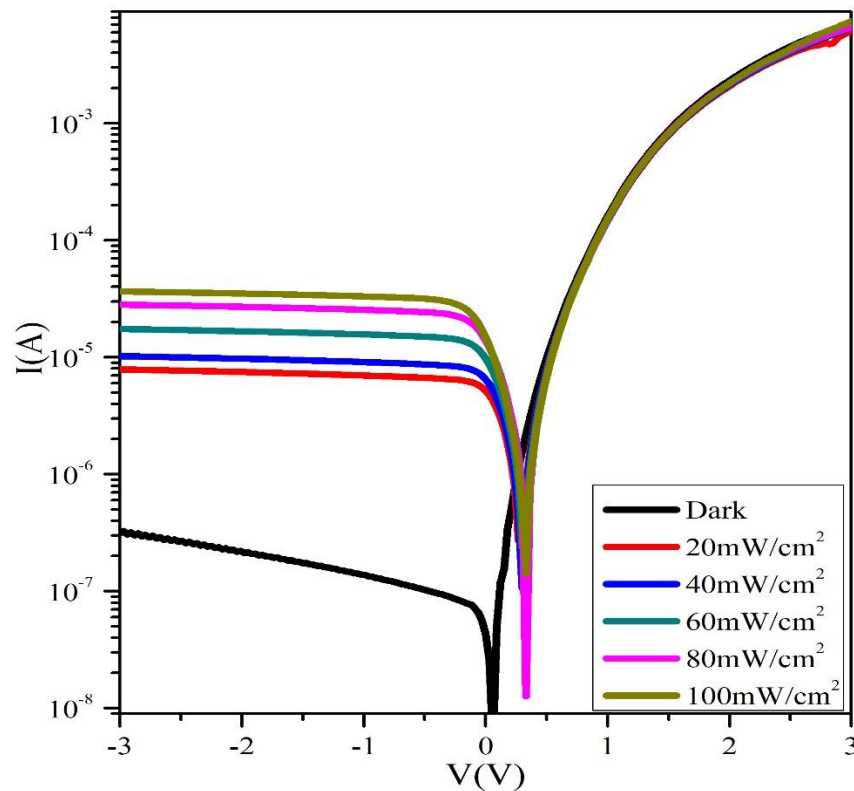


Figure 2: Current-voltage plot of $\text{Cu}_2\text{NiSnS}_4$ quaternary functional photodiodes obtained under infrared illumination.

Current-time behaviors of the $\text{Cu}_2\text{NiSnS}_4$ quaternary functional photodetectors were presented in Figure 3. Current-time characterization of the photodiodes were performed under 100 mW/cm^2 infrared illumination. Infrared light was applied for 5 sec intervals. Infrared illumination was kept on for 5 min and then turned off for 5 sec. At 100 mW/cm^2 infrared illumination intensity, maximum photocurrent was measured. The maximum photocurrent was found to be $3.1 \times 10^5 \text{ A}$. Shutting off the illumination resulted in a rapid cut off in the measured current. Repeated cycles

give similar and successful results. It was seen that $\text{Cu}_2\text{NiSnS}_4$ quaternary functional photodetectors were susceptible to infrared light.

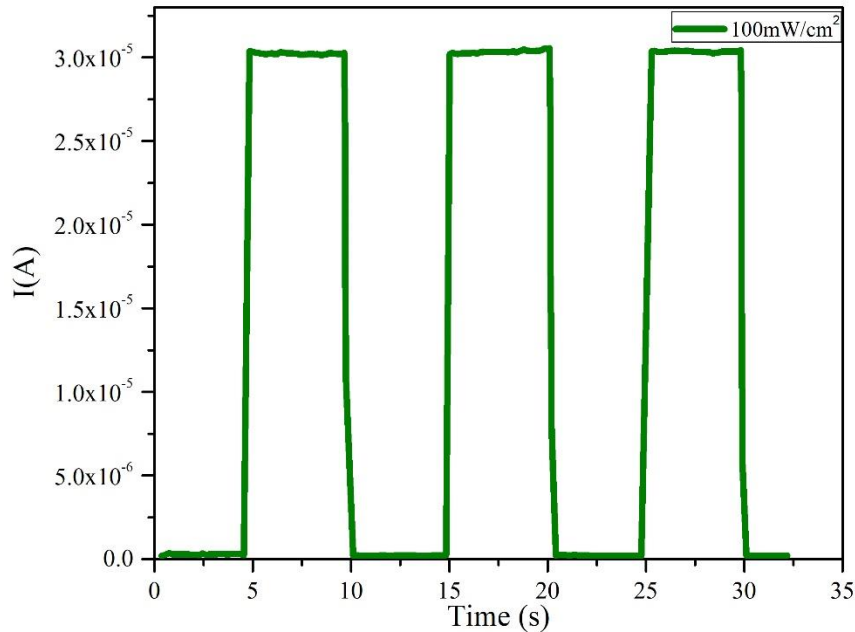


Figure 3: Current-time behaviors of $\text{Cu}_2\text{NiSnS}_4$ quaternary functional photodiodes.

Current-voltage and current-time characteristics was utilized to calculate the (n) ideality factor, (ϕ_b) barrier height, (R_s) photosensitivity and saturation constants. To calculate the photoelectric characteristics of the $\text{Cu}_2\text{NiSnS}_4$ quaternary functional photodetectors, thermionic emission theory was used [6], [33].

$$I=I_o\left[\exp\left(\frac{q(V-IR_s)}{nkT}\right)-1\right] \quad (1)$$

Formula above was used in the barrier height (ϕ_b) and ideality factor (n) calculation where n is ideality factor, T is absolute temperature, q is the charge of electron, k is Boltzman constant, I_o is backward bias current, R_s is serial resistance and V is applied voltage. I_o is calculated using Eq (2).

$$I_o=AA^*T^2\exp\left(-\frac{q\phi_b}{kT}\right) \quad (2)$$

In Eq 2, A is the surface area of the diode, ϕ_b is the barrier height, A^* is the Richardson constant that is $32 \text{ A/cm}^2\text{K}^2$. The slope and the intercept of the forward bias $\ln(I)$ vs. voltage (V) plot yield values for n and Φ_b , respectively. Table 1 represents the results exploited using thermionic emission theory. Ideality factor (n) was found to be 5.16. The expected value for the ideality factor is 1. However, there are many cases in the literature where ideality factor is greater than 1.

Barrier height of the $\text{Cu}_2\text{NiSnS}_4$ quaternary functional photodiodes were calculated as 0.466 eV which is within the range that were reported for the metallic thin film-based photodiodes in the literature. Barrier heights of Fe doped ZnO photodiodes were found to be between 0.45 eV and 0.51 eV [11]. Barrier height of Pt:carbon composite diodes were reported as 0.52 eV and barrier height for ZnO: carbon photodiodes were reported as 0.46 eV [1], [2].

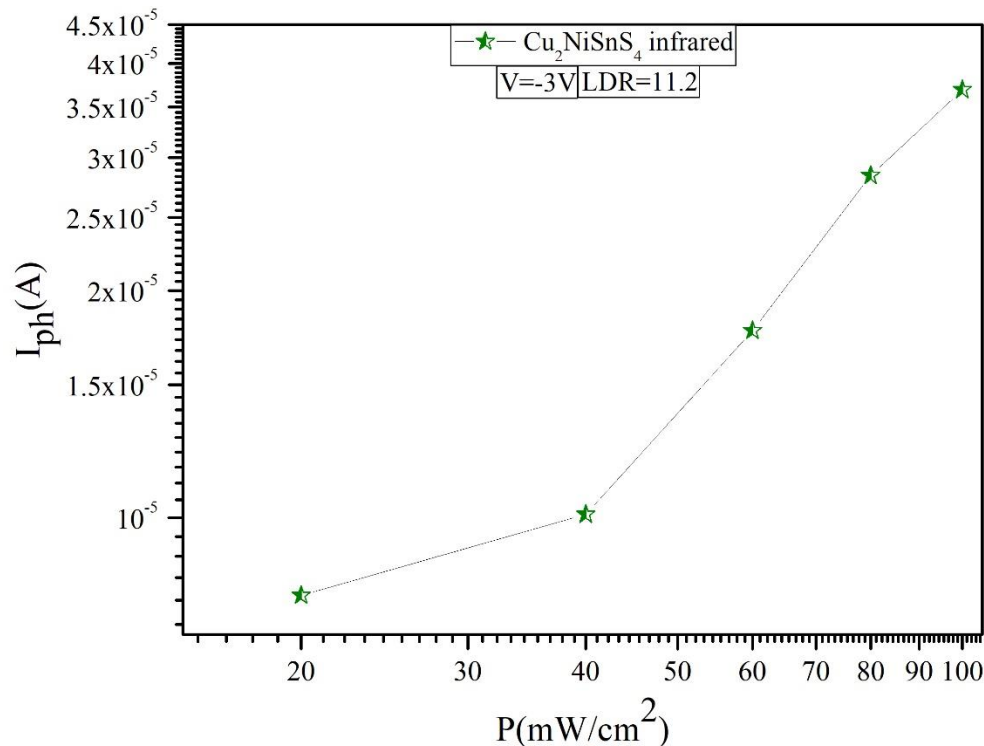


Figure 4: Photocurrent-Illumination intensity plot of $\text{Cu}_2\text{NiSnS}_4$ photodetectors.

Table 1: barrier height (ϕ_b), ideality factor (n), photosensitivity (R) and saturation current (I_0) $\text{Cu}_2\text{NiSnS}_4$ photodiodes.

Photodiode	n	R(A/W)	ϕ_b (eV)	I_0 (A)
IR Light	5.16	4.90×10^{-5}	0.466	3.25×10^{-4}

Photosensitivity of $\text{Cu}_2\text{NiSnS}_4$ quaternary functional photodetectors were assessed. In the calculation of the $\text{Cu}_2\text{NiSnS}_4$ quaternary functional photodetectors photocurrent is graphed as a function of illumination intensity. Photocurrent-illumination intensity characteristics was illustrated in Figure 4. Formula in Eq. 3 was used in the calculation

$$I_{PH} = KP^m \quad (3)$$

P represents the illumination and m is a constant in the Eq. 3.

Photocurrent-infrared illumination plot represents data obtained between $20\text{mW}/\text{cm}^2$ $100\text{mW}/\text{cm}^2$. Figure demonstrates that diodes respond to infrared light. Furthermore, enhanced photocurrent was seen for enhanced illumination intensity. $100\text{mW}/\text{cm}^2$ infrared illumination represents the highest photocurrent as $3.7 \cdot 10^{-5}$ A. LDR(Linear Dynamic Rate) was evaluated utilizing the $I_{Ph} - P$ slope. LDR of the $\text{Cu}_2\text{NiSnS}_4$ quaternary functional photodetectors were found to be 11.2 dB.

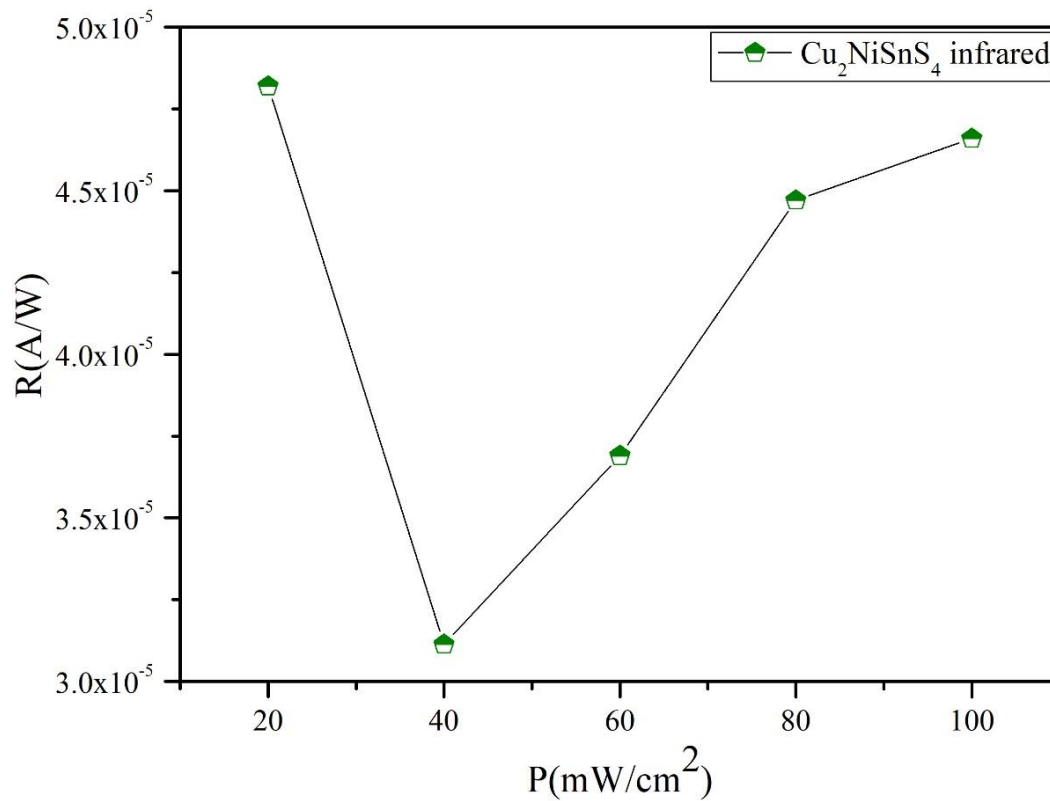


Figure 5: Photosensitivity-Illumination intensity plot of $\text{Cu}_2\text{NiSnS}_4$ photodetectors.

Photosensitivity (R) of $\text{Cu}_2\text{NiSnS}_4$ quaternary functional photodetectors were evaluated using the equation below

$$R = \frac{(I_p - I_d)}{PA} \quad (4)$$

where I_d , A, P, and I_p are dark current, surface area, illumination intensity and photocurrent, respectively.

Photosensitivity (R) of $\text{Cu}_2\text{NiSnS}_4$ photodetectors were demonstrated in Figure 5. 20 mW/cm^2 was found to be the highest photosensitivity which was $4.90 \cdot 10^{-5}$ A/W. The lowest photosensitivity for $\text{Cu}_2\text{NiSnS}_4$ photodetectors was measured at 100mW/cm^2 . Photosensitivity of the $\text{Cu}_2\text{NiSnS}_4$ photodetectors show diminishing trend with diminishing illumination.

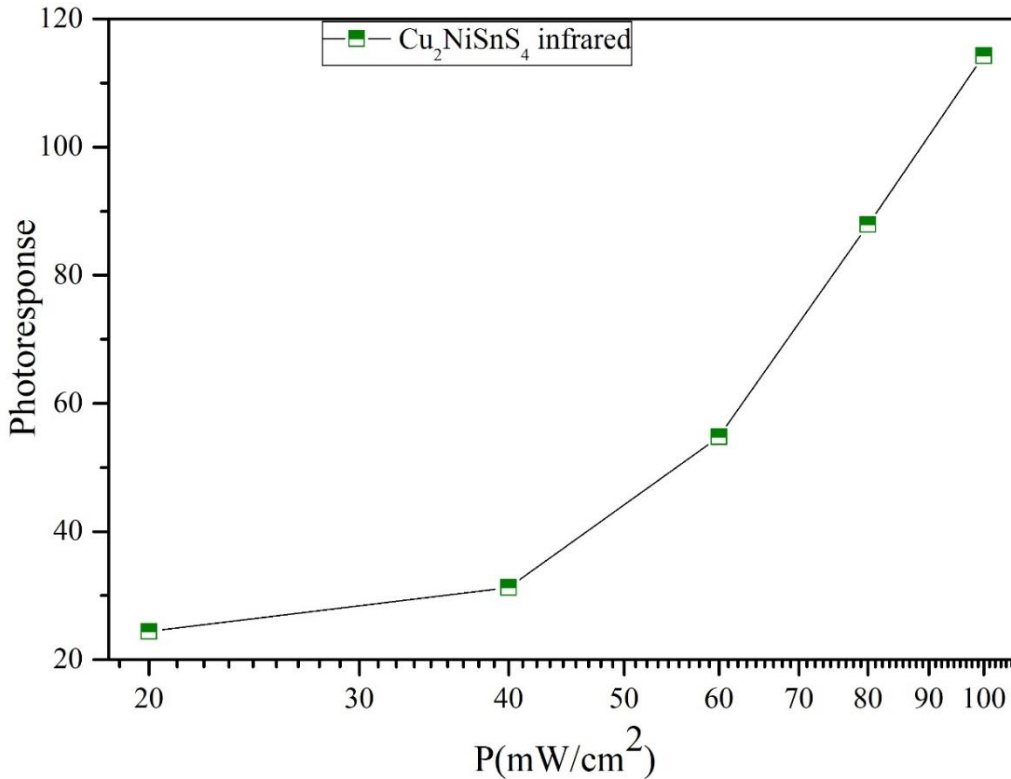


Figure 6: Photoresponse-Illumination plot of $\text{Cu}_2\text{NiSnS}_4$ quaternary functional photodetector.

Photoresponse behaviour of $\text{Cu}_2\text{NiSnS}_4$ photodetectors was presented in Figure 6. I-t characteristics was used in the assessment of photoresponse behaviours. Enhancing photoresponse characteristics was seen with augmenting infrared illumination. 100mW/cm^2 was found to be the value where the highest photoresponse was obtained. Photoresponse value was measured as $0.33 \cdot 10^2$ for 100mW/cm^2 infrared illumination. Photoresponse behaviours illustrated that $\text{Cu}_2\text{NiSnS}_4$ quaternary functional photodetectors were responsive to infrared light and a good candidate for sensing implications such as infrared sensors, infrared tracking devices or photodiodes.

4. CONCLUSION

$\text{Cu}_2\text{NiSnS}_4$ nanoparticles were prepared using sol-gel method. $\text{Cu}_2\text{NiSnS}_4$ was spin coated to fabricate $\text{Cu}_2\text{NiSnS}_4$ photodiodes. Surface properties of the $\text{Cu}_2\text{NiSnS}_4$ quaternary functional photodetectors were evaluated using electron microscopy. Current-voltage and current-time

behaviours of the $\text{Cu}_2\text{NiSnS}_4$ quaternary functional photodetectors revealed that diodes are responsive to infrared light. Ideality factor, saturation current, and barrier height characteristics were evaluated. We benefit from thermionic emission theory in our assessment and calculations. Results indicate that photosense, photoresponse characteristics of the $\text{Cu}_2\text{NiSnS}_4$ quaternary functional photodetectors have good infrared sensing properties. They have great potential to be used in infrared tracking device technologies.

REFERENCES

- [1] M. Koç *et al.*, “Electrical characterization of solar sensitive zinc oxide doped-amorphous carbon photodiode,” *Optik.*, C 178, S 316–326, 2019.
- [2] N. Aslan *et al.*, “Ti doped amorphous carbon (Al/Ti-a:C/p-Si/Al) photodiodes for optoelectronic applications,” *J. Mol. Struct.*, C 1155, S 813–818, 2018.
- [3] N. Aslan, N. Başman, and O. Uzun, “Investigation of Optical, Morphological and Mechanical Properties of Diamond-Like Carbon Films Synthesized by Electrodeposition Technique Using Formic Acid,” *Int. J. Pure Appl. Sci.*, C 2, S 57–63, 2016.
- [4] A. Dere, M. Soylu, and F. Yakuphanoglu, “Solar light sensitive photodiode produced using a coumarin doped bismuth oxide composite,” *Mater. Sci. Semicond. Process.*, C 90, S 129–142, 2019.
- [5] A. Mekki *et al.*, “Graphene controlled organic photodetectors,” *Synth. Met.*, C 217, S 43–56, 2016.
- [6] N. Aslan, N. Başman, O. Uzun, M. Erkovan, and F. Yakuphanoglu, “The effects of deposition potential on the optical, morphological and mechanical properties of DLC films produced by electrochemical deposition technique at low,” *Mater. Sci.*, C 37, no. 2, S 166–172, 2019.
- [7] A. A. Hendi and F. Yakuphanoglu, “Graphene doped TiO_2 /p-silicon heterojunction photodiode,” *J. Alloys Compd.*, C 665, S 418–427, 2016.
- [8] A. Karabulut *et al.*, “Silicon based photodetector with Ru(II) complexes organic interlayer,” *Mater. Sci. Semicond. Process.*, C 91, S 422–430, 2019.
- [9] B. Coskun, “Capacitance and Dielectric Properties of Mn Doped CdO Photodetectors,” *J. Mater. Electron. DEVICES*, C 1, no. 1, S 65–71, 2019.
- [10] B. Coskun, T. Asar, U. Akgul, K. Yildiz, and Y. Atici, “Investigation of structural and electrical properties of Zirconium dioxide thin films deposited by reactive RF sputtering

- technique,” *Ferroelectrics*, C 502, no. 1, S 147–158, 2016.
- [11] B. Coşkun *et al.*, “Optoelectrical properties of Al/p-Si/Fe:N doped ZnO/Al diodes,” *Thin Solid Films*, C 653, S 236–248, 2018.
- [12] T. Rezkallah, I. Djabri, M. M. Koç, M. Erkovan, Y. Chumakov, and F. Chemam, “Investigation of the electronic and magnetic properties of Mn doped ZnO using the FP-LAPW method,” *Chinese J. Phys.*, C 55, no. 4, S 1432–1440, 2017.
- [13] R. Topkaya, M. Erkovan, A. Öztürk, O. Öztürk, B. Akta, and M. Özdemir, “Ferromagnetic resonance studies of exchange coupled ultrathin Py/Cr/Py trilayers,” *J. Appl. Phys.*, C 108, no. 2, 2010.
- [14] M. Erkovan *et al.*, “Probing Exchange Bias Properties of Pt x Co1-x /Pt/CoO Films,” *J. Supercond. Nov. Magn.*, C 29, no. 1, S 163–168, 2016.
- [15] F. Yakuphanoglu, “Transparent metal oxide films based sensors for solar tracking applications,” *Compos. Part B Eng.*, C 92, S 151–159, 2016.
- [16] A. Tataroğlu, A. A. Al-Ghamdi, F. El-Tantawy, W. A. Farooq, and F. Yakuphanoglu, “Analysis of interface states of FeO-Al₂O₃ spinel composite film/p-Si diode by conductance technique,” *Appl. Phys. A*, C 122, no. 3, S. 220, 2016.
- [17] F. Yakuphanoglu, “Preparation of nanostructure Ni doped CdO thin films by sol gel spin coating method,” *J. Sol-Gel Sci. Technol.*, C 59, no. 3, S 569–573, 2011.
- [18] A. Gencer Imer, “Investigation of Al doping concentration effect on the structural and optical properties of the nanostructured CdO thin film,” *Superlattices Microstruct.*, C 92, S 278–284, 2016.
- [19] S. Dugan, M. M. Koç, and B. Coşkun, “Structural, electrical and optical characterization of Mn doped CdO photodiodes,” *J. Mol. Struct.*, C 1205, p. 127235, 2019.
- [20] B. A. H. Ameen, A. Yildiz, W. A. Farooq, and F. Yakuphanoglu, “Solar Light Photodetectors Based on Nanocrystalline Zinc Oxide Cadmium Doped/p-Si Heterojunctions,” *Silicon*, C 11, no. 1, S 563–571, 2019.
- [21] S. H. Güler, M. Boyrazlı, Ö. Başgöz, and F. Yakuphanoglu, “The effects of nanoporous Fe₂O₃ synthesized via mechano-thermal process on electrical and optical properties of zinc oxide,” *Phys. B Condens. Matter*, C 547, S 120–126, 2018.
- [22] S. Rondiya, N. Wadnerkar, Y. Jadhav, S. Jadkar, S. Haram, and M. Kabir, “Structural, Electronic, and Optical Properties of Cu₂NiSnS₄: A Combined Experimental and Theoretical Study toward Photovoltaic Applications,” *Chem. Mater.*, C 29, no. 7, S 3133–3142, 2017.



- [23] F. Ozel, E. Aslan, B. Istanbulu, O. Akay, and I. Hatay Patir, “Photocatalytic hydrogen evolution based on Cu₂ZnSnS₄, Cu₂NiSnS₄ and Cu₂CoSnS₄ nanocrystals,” *Appl. Catal. B Environ.*, C 198, S 67–73, 2016.
- [24] J. Y. Chane-Ching, A. Gillorin, O. Zaberca, A. Balocchi, and X. Marie, “Highly-crystallized quaternary chalcopyrite nanocrystals via a high-temperature dissolution-reprecipitation route,” *Chem. Commun.*, C 47, no. 18, S 5229–5231, 2011.
- [25] F. Al-Hazmi and F. Yakuphanoglu, “Cu₂ZnSnS₄:graphene oxide nanocomposites based photoresponse devices,” *J. Alloys Compd.*, C 653, S 561–569, 2015.
- [26] M. M. K. Mustafa İlhan, “Infrared Sensing Properties of Quaternary Cu₂CoSnS₄ Photodetectors,” *J. Mater. Electron. DEVICES*, C 1, no. 1, S 19–24, 2020.
- [27] H. J. Chen, S. W. Fu, T. C. Tsai, and C. F. Shih, “Quaternary Cu₂NiSnS₄ thin films as a solar material prepared through electrodeposition,” *Mater. Lett.*, C 166, S 215–218, 2016.
- [28] M. Courel, J. A. Andrade-Arvizu, and O. Vigil-Galán, “Loss mechanisms influence on Cu₂ZnSnS₄/CdS-based thin film solar cell performance,” *Solid. State. Electron.*, C 111, S 243–250, 2015.
- [29] A. Rogalski, “Infrared detectors: An overview,” *Infrared Phys. Technol.*, C 43, no. 3–5, S 187–210, 2002.
- [30] E. Bilgilişoy, S. Özden, E. Bakali, M. Karakaya, and Y. Selamet, “Characterization of CdTe Growth on GaAs Using Different Etching Techniques,” *J. Electron. Mater.*, C 44, no. 9, S 3124–3133, 2015.
- [31] S. Özden and M. M. Koc, “Spectroscopic and microscopic investigation of MBE-grown CdTe (211)B epitaxial thin films on GaAs (211)B substrates,” *Appl. Nanosci.*, C 8, no. 4, S 891–903, 2018.
- [32] S. Özden and M. M. Koç, “Wet-chemical etching of GaAs(211)B wafers for controlling the surface properties,” *Int. J. Surf. Sci. Eng.*, C 13, no. 2/3, p. 79, 2019.
- [33] A. Turut, A. Karabulut, K. Ejderha, and N. Biyikli, “Capacitance-conductance-current-voltage characteristics of atomic layer deposited Au/Ti/Al₂O₃/n-GaAs MIS structures,” *Mater. Sci. Semicond. Process.*, C 39, S 400–407, 2015.